USM3D-ME Revised SA-neg Implementation and Assessment for DPW-VII Solutions

Boris Diskin
National Institute of Aerospace

Mohagna Pandya, Brent Pomeroy, and Taylor Kate Boyett
NASA Langley Research Center

Special Session APA – 06: 7th AIAA CFD Drag Prediction Workshop
2023 AIAA Aviation Forum, June 12, 2023

This material is a work of the U.S. Government and is not subject to copyright protection in the United States

Outline

- **Background**
- **USM3D-ME Overview**
- **SA-neg Turbulence Model**
  - Partial Differential Equation (PDE)
  - Discretization
- **Required DPW-VII Cases**
  - Case 1a: Grid Convergence Study for Re=20 million
  - Case 2a: Alpha Sweep for Re=20 million
  - Case 3: Reynolds Number Sweep
- **Conclusions**

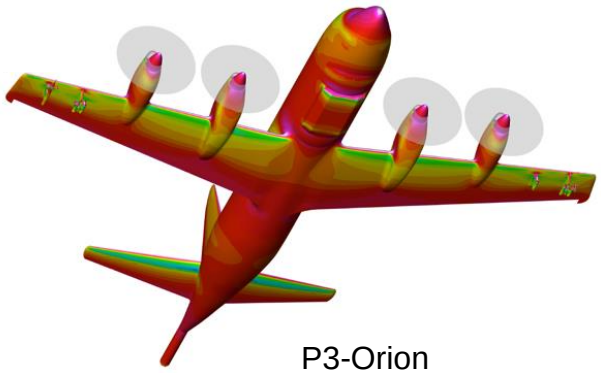
Background

- **Drag Prediction Workshop (DPW) series**
  - sponsored by AIAA APA TC
  - seven workshops since 2001
  - computational predictions of aerodynamic forces and moments for industry-relevant cases
  - code-to-code spread between drag predictions for a wing-body configuration reduced from 270 counts (DPW-I) to less than 10 counts (DPW-VI)
- **Approach**
  - rigorous statistical analysis
  - Common Research Model (CRM)
  - fine grids with $O(10^8)$ degrees of freedom
  - detailed guidelines for grid generation
  - code verification using the NASA Turbulence Modeling Resource (TMR) solutions
- **Further improvements needed**
  - focus on iterative convergence

AIAA JoA 40(5) 2003, AIAA JoA 42(5) 2005, AIAA JoA 45(3) 2008, AIAA JoA 51(4) 2014, AIAA JoA 55(4) 2017

Mixed-Element USM3D (USM3D-ME)

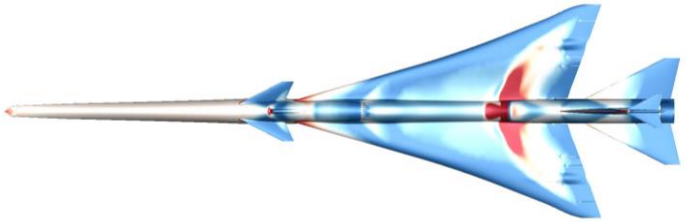
- **Builds on rich legacy of USM3D tetrahedral grid flow solver**
- **Cell-centered, finite-volume, unstructured-grid flow solver**
  - second-order spatial accuracy
  - Spalart-Allmaras (SA) turbulence model (standard, negative, QCR2000, rotation/curvature correction)
  - DPW-VII solutions: SA-neg-QCR2000 with 1st-order convection term
- **Upwind spatial discretization for mean flow inviscid flux**
  - cell gradients using Green-Gauss method and nodal solutions
  - options for flux functions: FDS, HLLC, LDFSS, FVS, HLLE, etc.
  - cell- and face-based gradient limiters: Barth-Jespersen, Venkatakrishnan, van Albada
  - DPW-VII solutions: Roe's FDS with no gradient limiters
- **Second-order diffusion**
  - face-gradients based on Mitchell's method



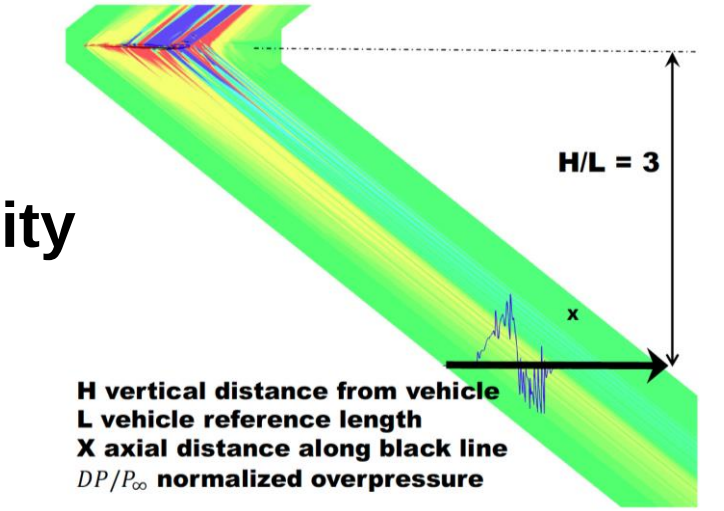
P3-Orion
Courtesy Craig Hunter (NASA LaRC)

USM3D-ME

- **Standard and specialized boundary conditions**
- **Force-term approach for simulation of propellers and other applications**
- **Time integration**
  - steady state with local time-stepping
  - implicit/explicit BDF2 for temporal accuracy
- **Rigid-body 6-DoF motion support**
- **Parallelized using MPI paradigm; excellent scalability**
- **Nonlinear iteration methods**
  - Preconditioner-Alone (PA); baseline solver technology
  - Hierarchical Adaptive Nonlinear Iteration Method (HANIM)
  - DPW-VII solutions: HANIM with maximum of 50 search directions



C608 Low Boom Flight Demonstrator
Pictures are courtesy Alaa Elmiligui (NASA LaRC)



AIAA 2013-2541, *AIAAJ* 54(9) 2016, *AIAAJ* 55(10) 2017, AIAA 2019-2333, *AIAAJ* 59(8) 2021, *AIAAJ* 59(11) 2021

SA-neg Turbulence Model - PDE

- **Standarad SA model**
  - eddy viscosity defined for positive working variable
  - working variables truncated to remain positive
    - can hinder iterative convergence
- **SA-neg model (negative variant) introduced in 2012** (ICCFD7-1902, 2012)
  - identical to standard SA model for positive working variable
    - allows working variable to become negative
  - zero eddy viscosity for negative working variable
  - modifies source and diffusion terms for negative working variable
  - improves iterative convergence
- **Theoretical foundation**
  - exact solution of SA-neg model PDE is bounded and positive (rigorous proof)
  - reproduces standard SA model PDE solution
  - requires positive diffusion coefficient

$$\left[\nabla \cdot \left((\nu + \tilde{\nu} f_n)\nabla\tilde{\nu}\right) + c_{b2}(\nabla\tilde{\nu} \cdot \nabla\tilde{\nu})\right]$$

SA-neg Turbulence Model – Discretization



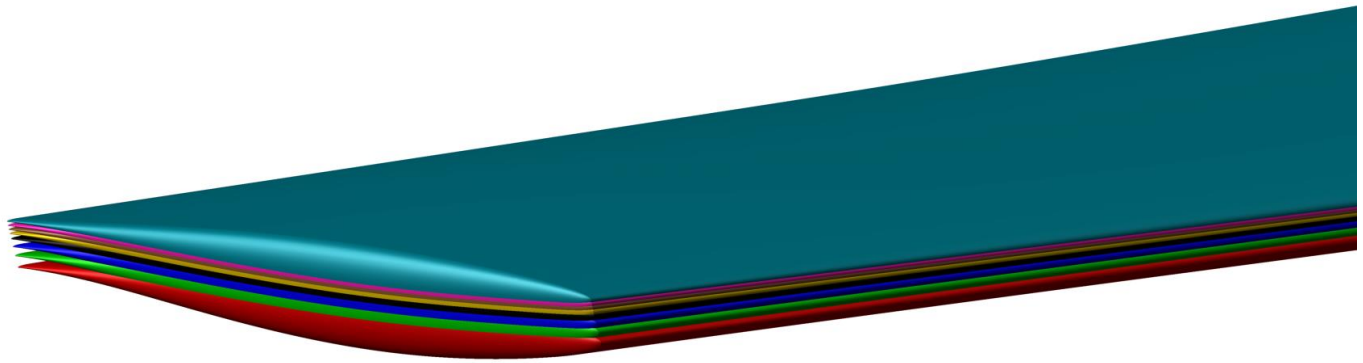
- **Function f_n ensures positive diffusion coefficient in SA-neg model PDE**
- **Original SA-neg model implementation**
  - solution evaluated at cell center
  - diffusion coefficient evaluated at cell boundary
  - may become negative even if cell-centered solutions/diffusion coefficients are positive
- **New SA-neg model implementation ensures positive diffusion coefficient**
  - details shown in paper
- **Theoretical analysis of discrete (zero-residual) SA-neg solution**
  - bounded and positive
  - reproduces exact discrete solution for standard SA model equation
- **Iterative convergence for DPW-7 cases**
  - improved robustness
  - machine-zero residuals achieved for all solutions on all grids

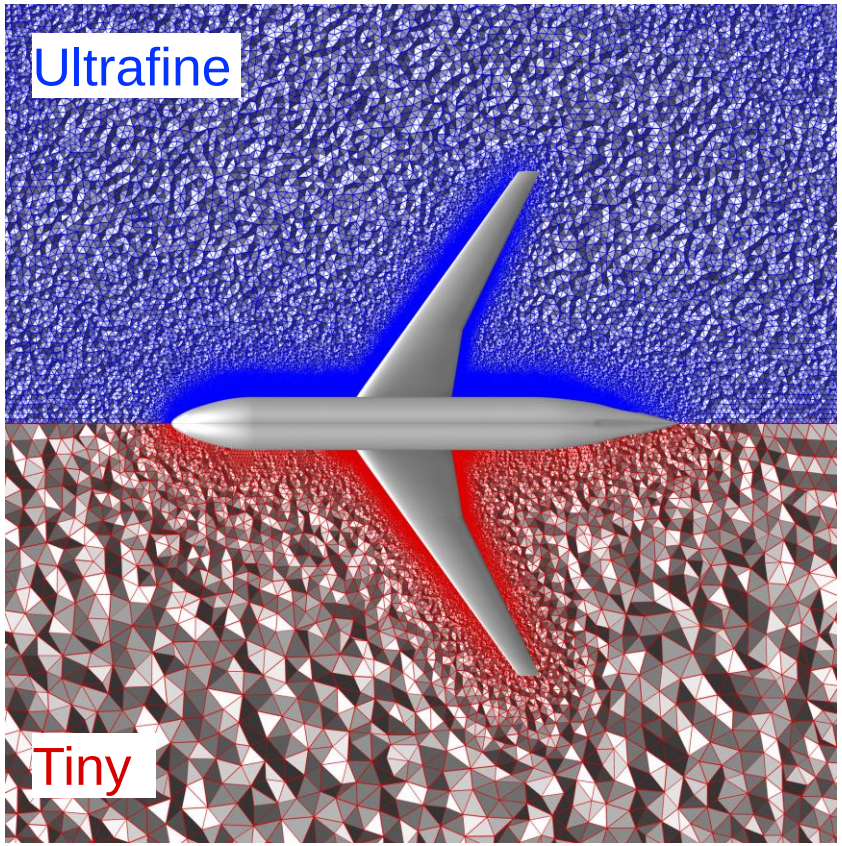
Grids

- **JAXA mixed-element grids**
  - grid convergence study performed on all grids
  - Cases 2a and 3a computed on medium grid

	Tiny	Coarse	Medium	Fine	Extrafine	Ultrafine
Level	L1	L2	L3	L4	L5	L6
Cell Count (Millions)	8.7	26.9	60.2	111.8	184.1	291.2

- **Low (LoQ) and high (HiQ) dynamic pressure aeroelastic deformations incorporated in grids**

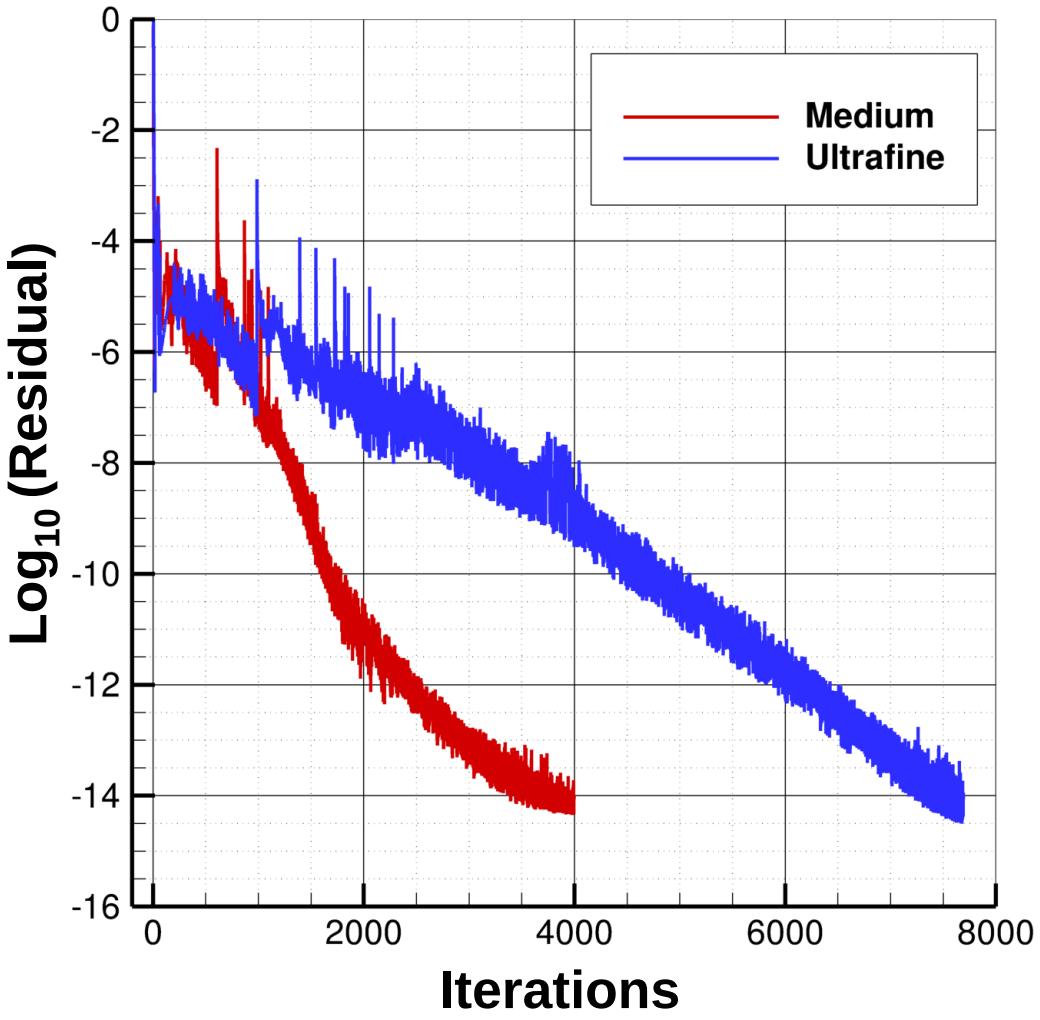


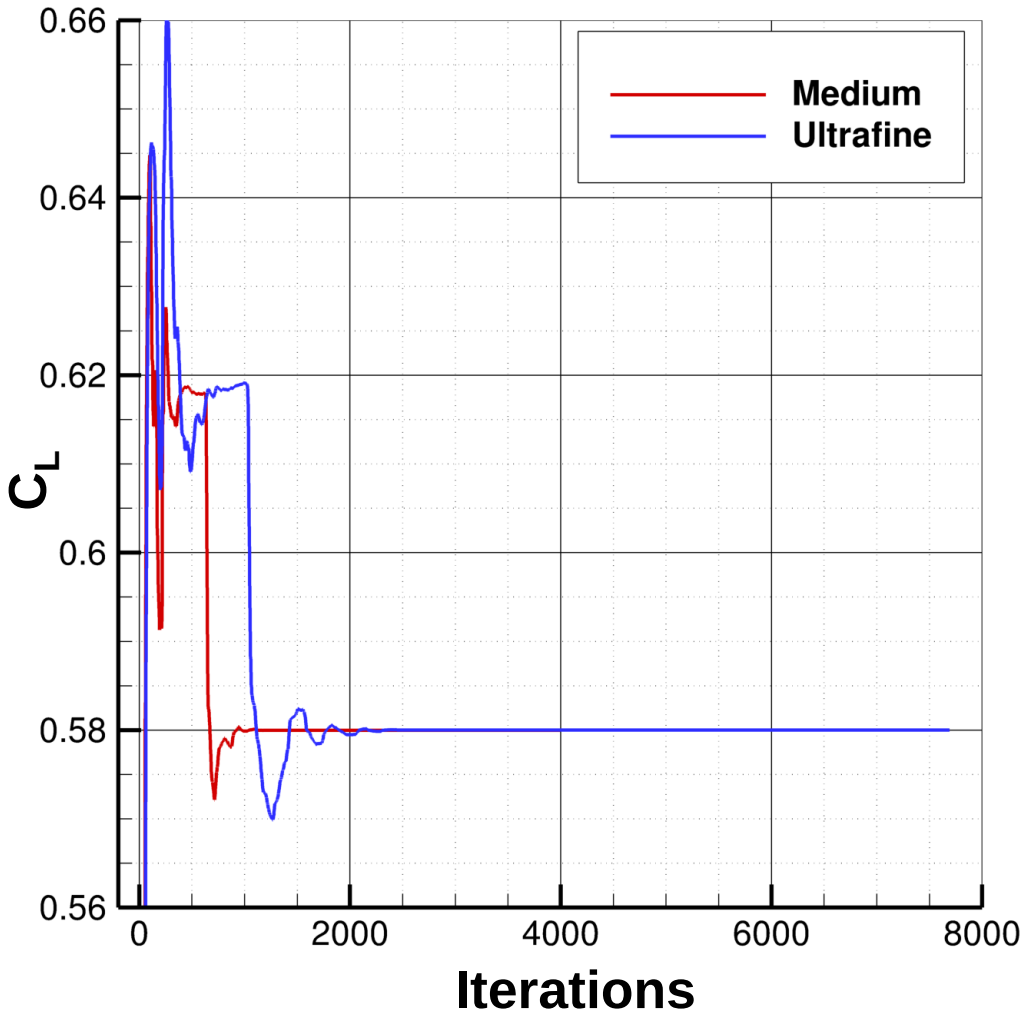


Case 1a: Grid Convergence Study

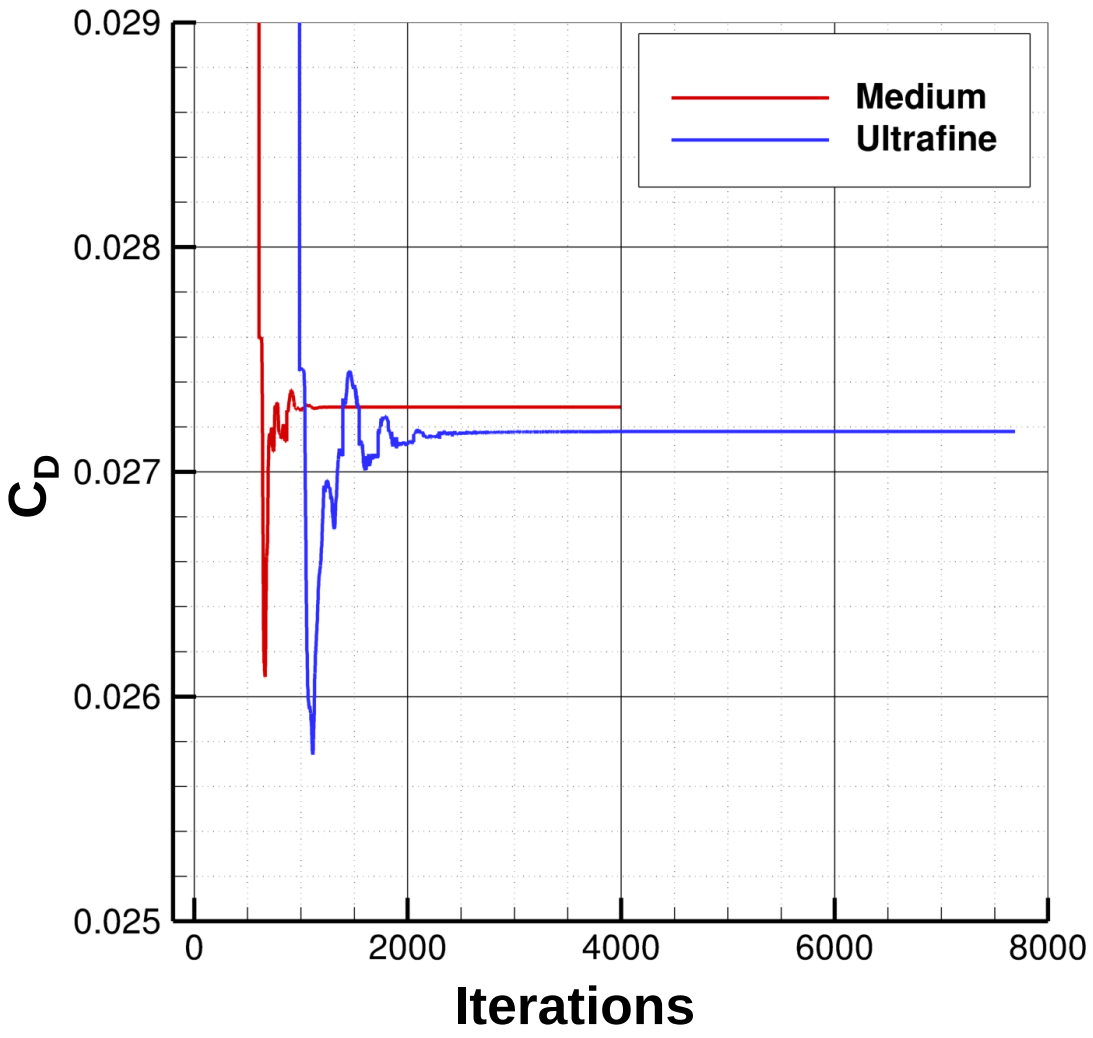
- **CRM wing-body configuration**
  - 3.0° LoQ aeroelastic deformation CRM geometry
- **Flow conditions**
  - Mach number: $M = 0.85$
  - Reynolds number: $Re = 20 \text{ million}$
  - fixed lift: $C_L = 0.58 \pm 0.0001$
  - reference temperature: $T_{ref} = -250\ °F$
- **USM3D-ME solutions computed on all six grids**
  - rapid iterative convergence from HANIM methodology
  - solution residuals reduced below 1.0E-13
- **C_L-matching mode**
  - angle of attack perturbed automatically to match prescribed C_L within the tolerance limits
  - angle of attack adjusted after residuals are reduced by 1.5 orders of magnitude

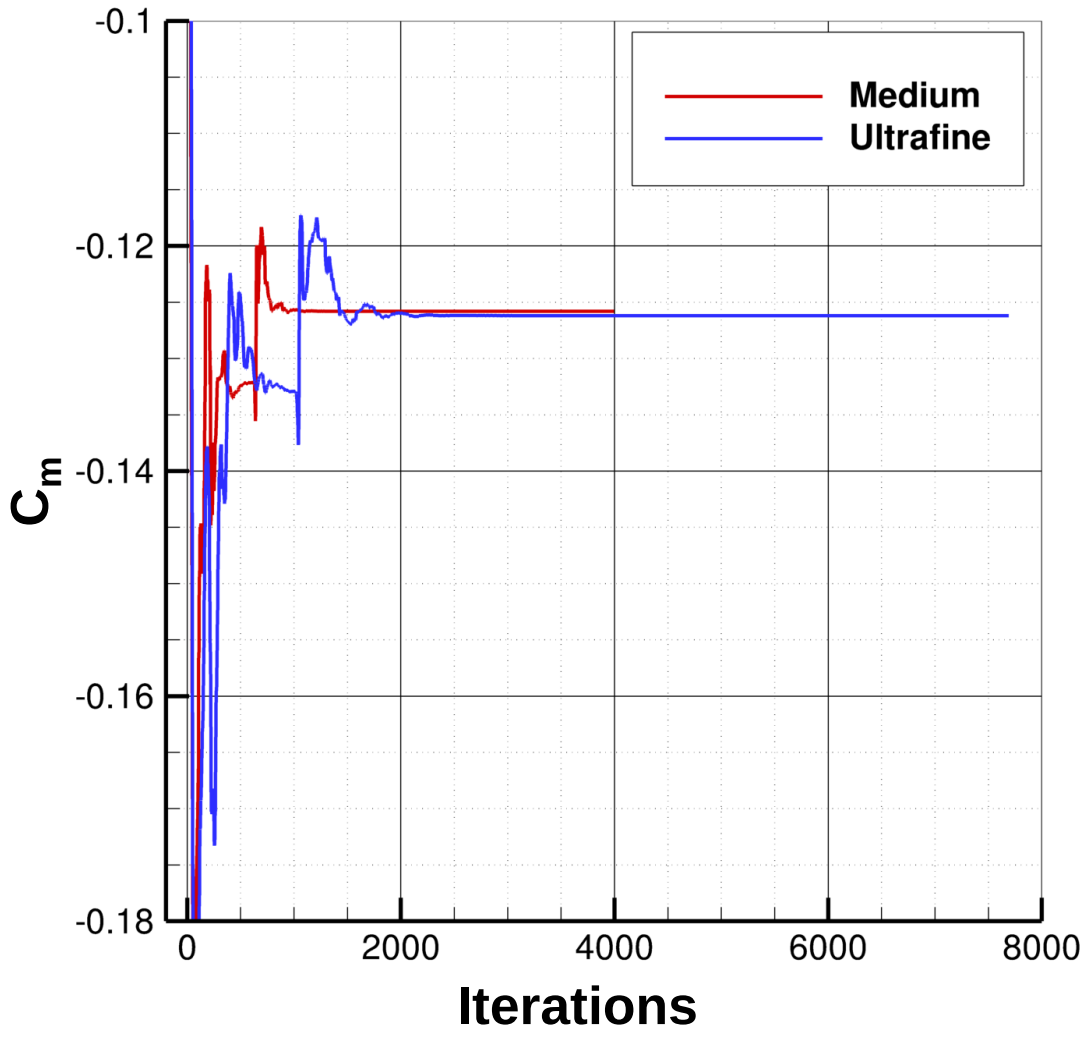
Case 1a: Iterative Convergence



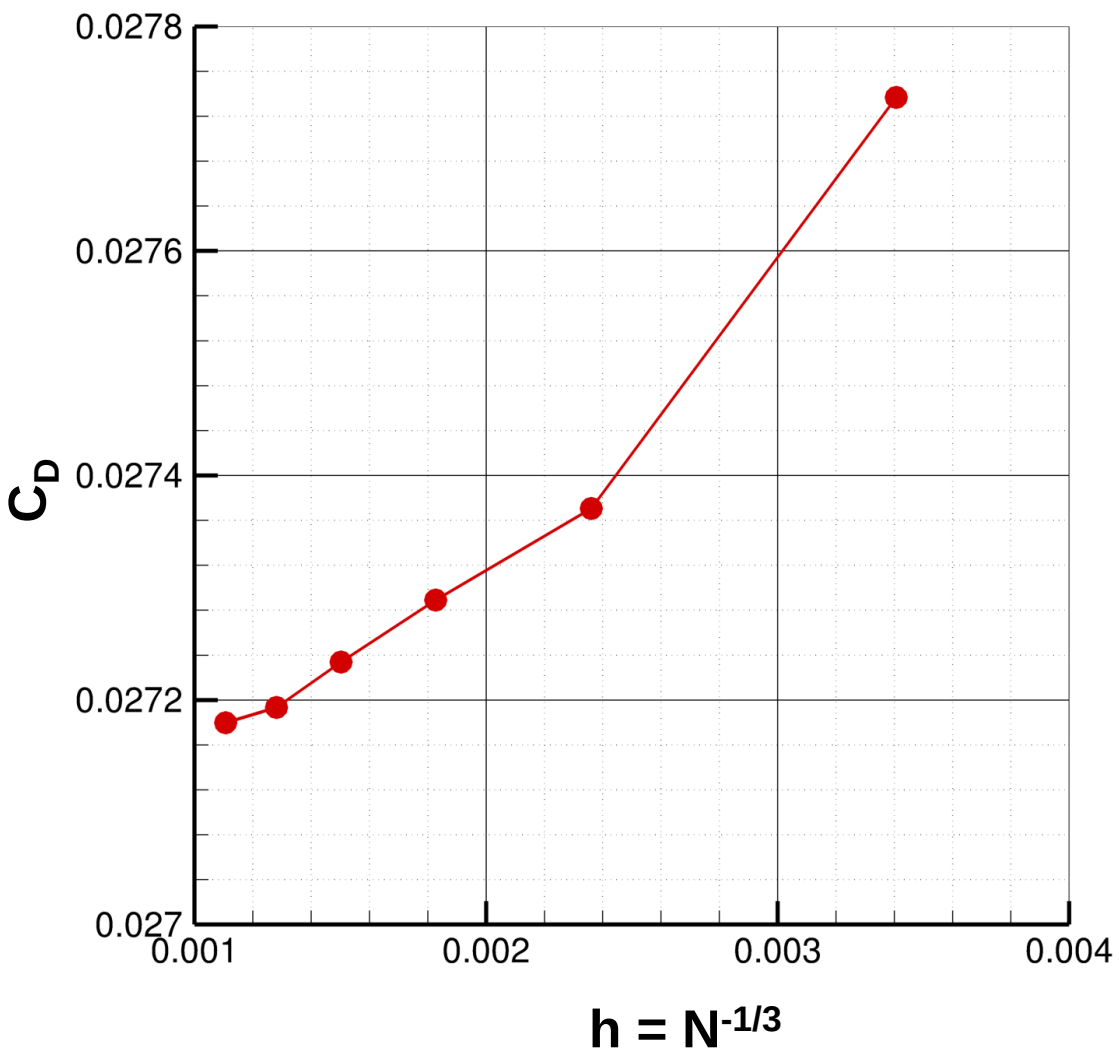


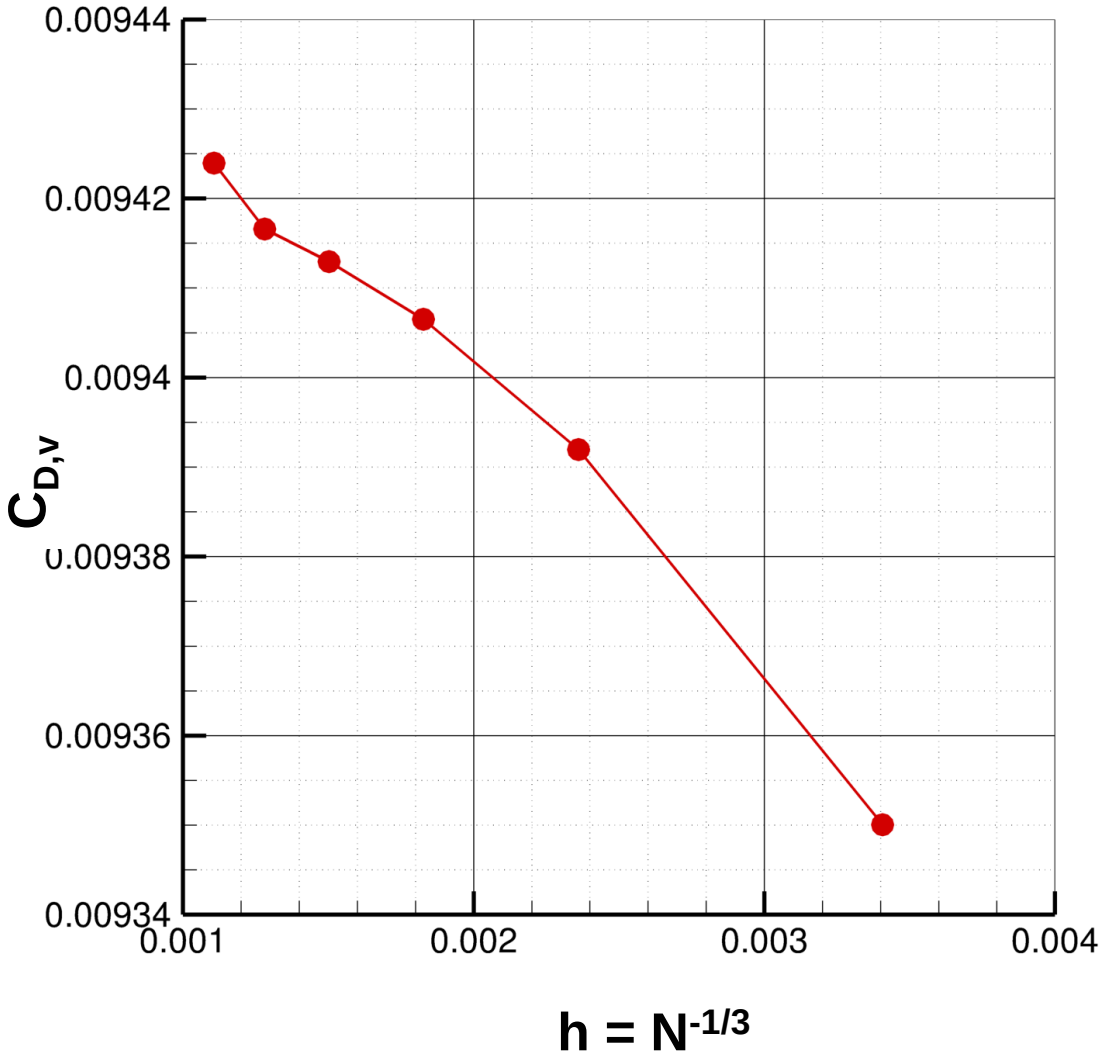
Case 1a: Iterative Convergence (cont.)



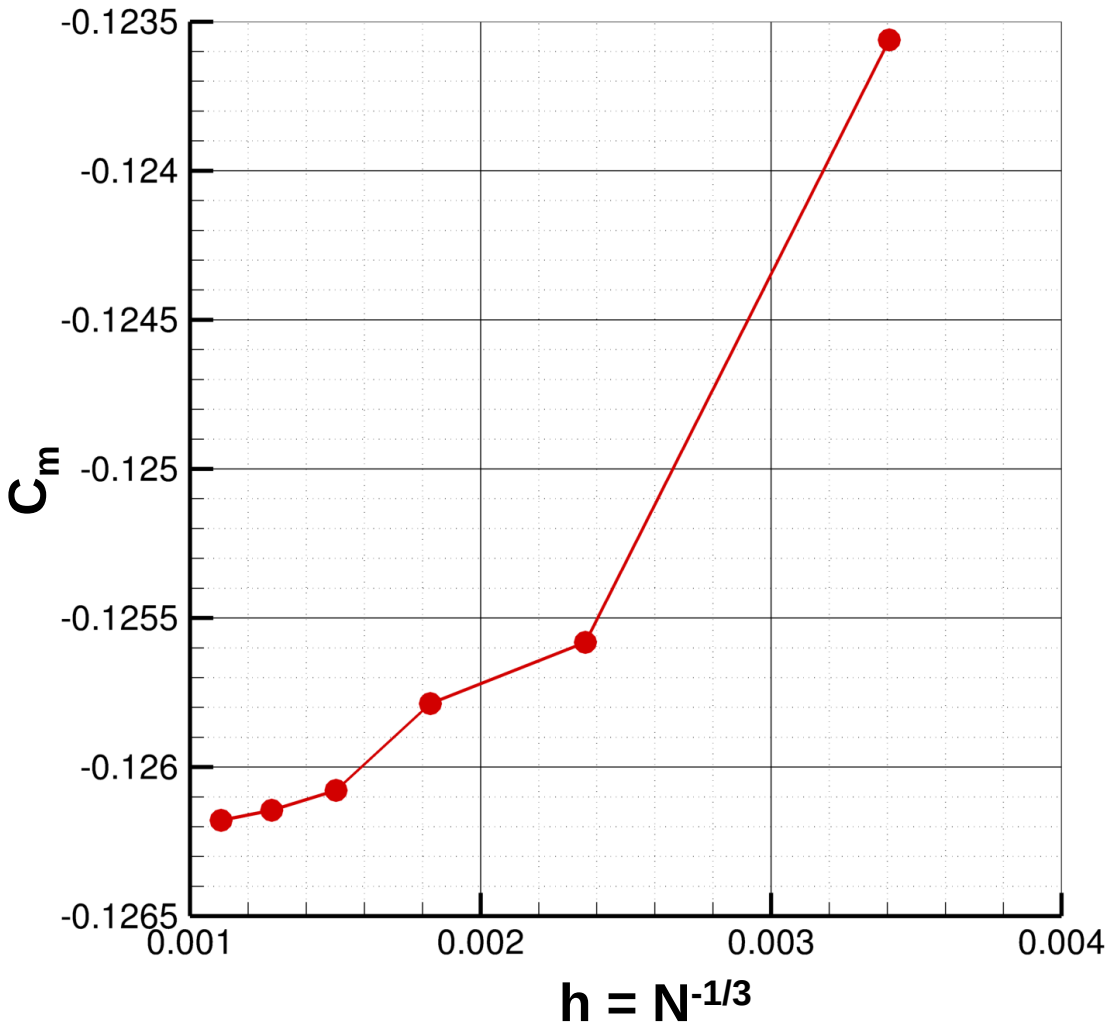


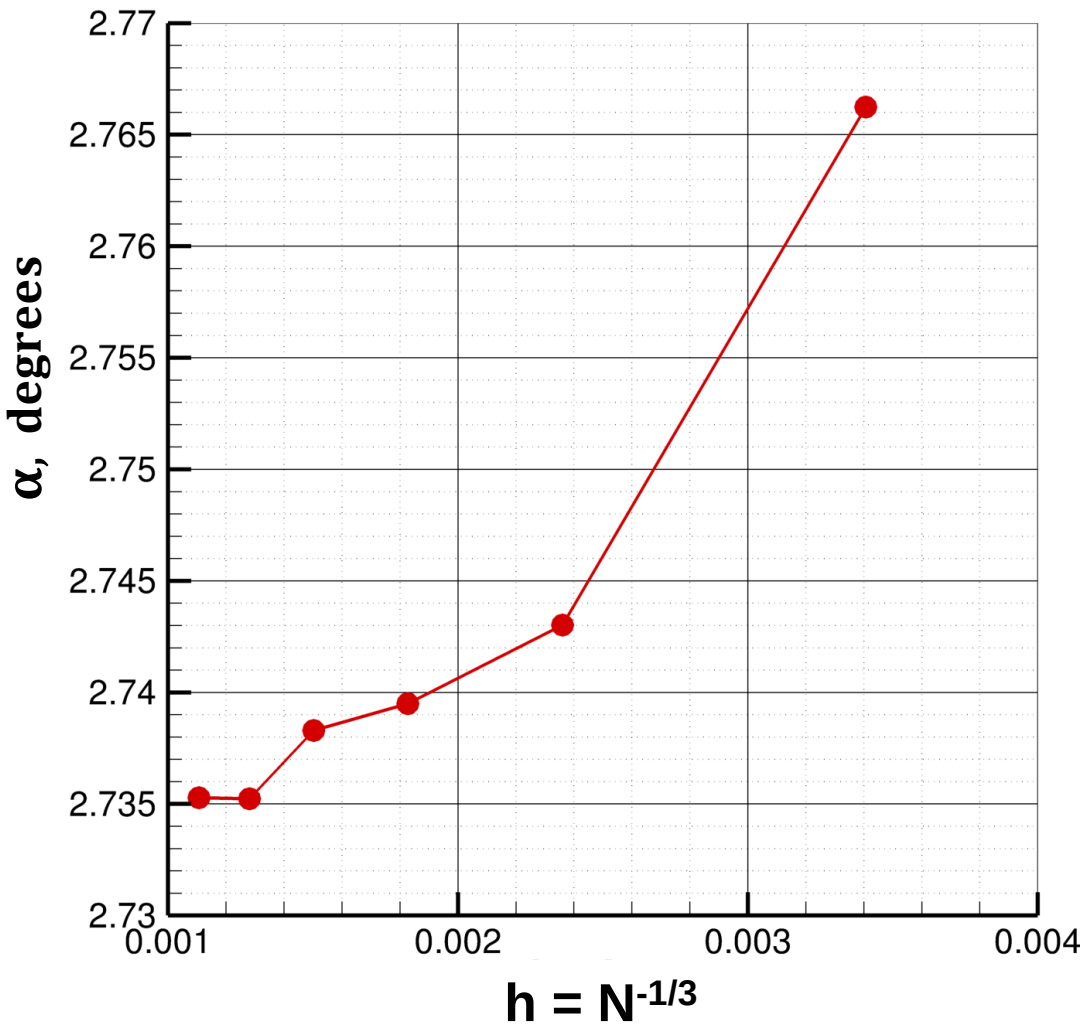
Case 1a: Grid Convergence





Case 1a: Grid Convergence (cont.)

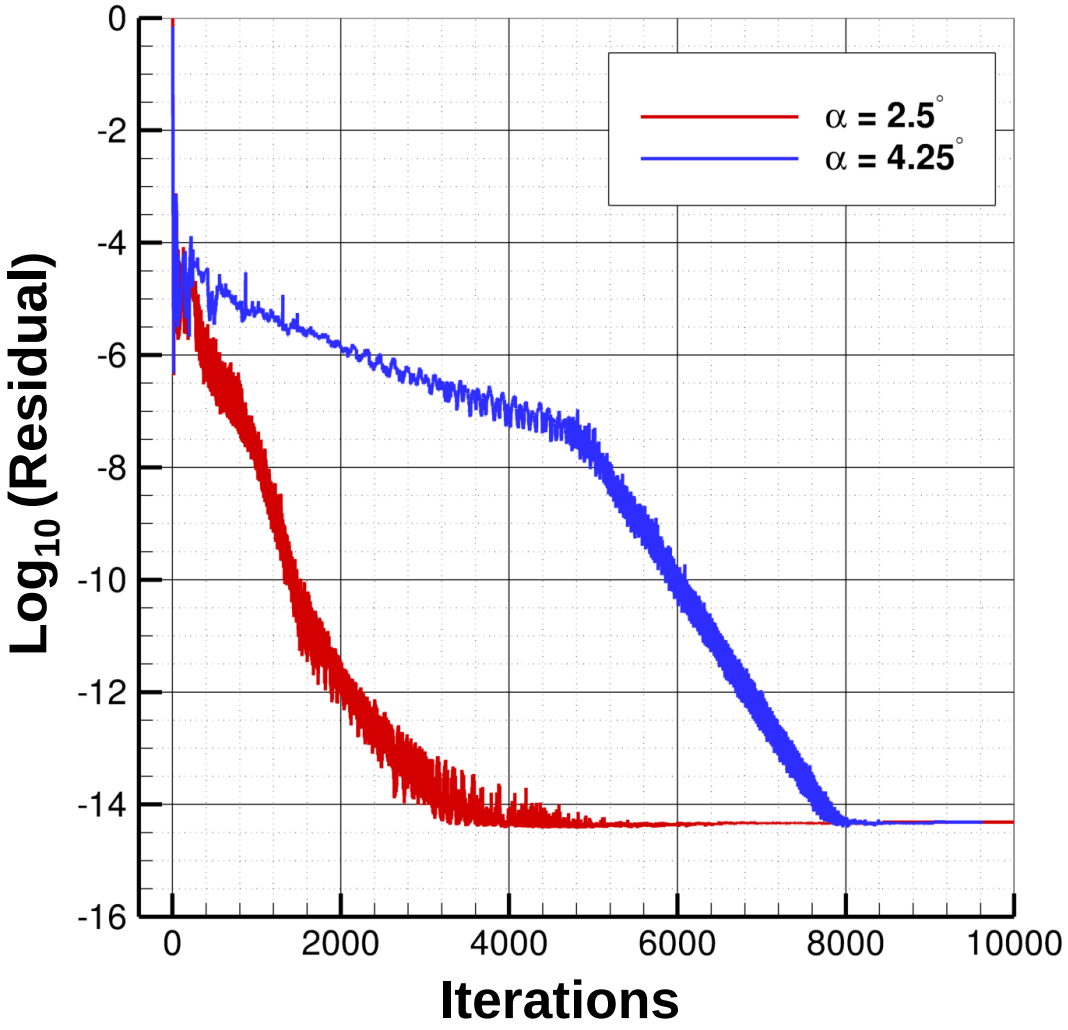


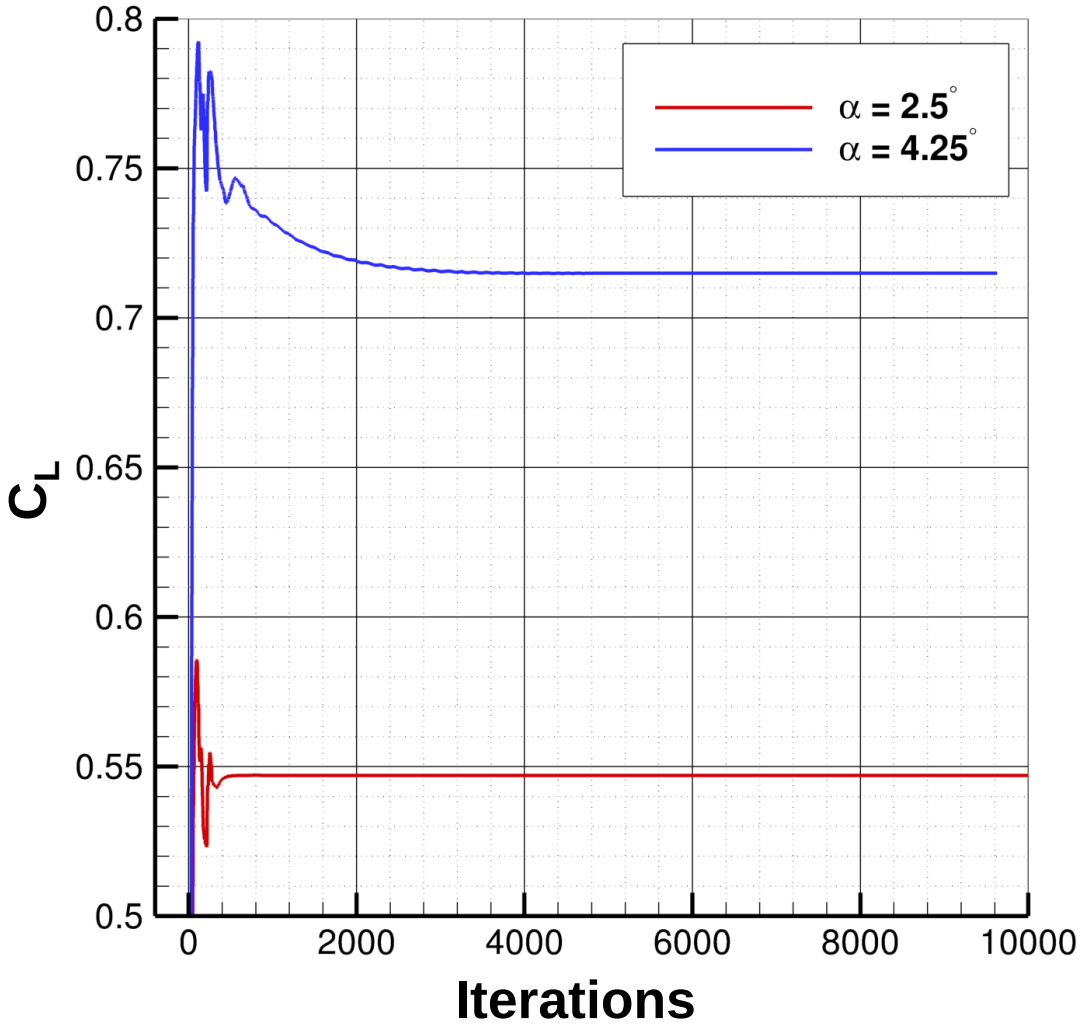


Case 2a: Angle-of-Attack Sweep

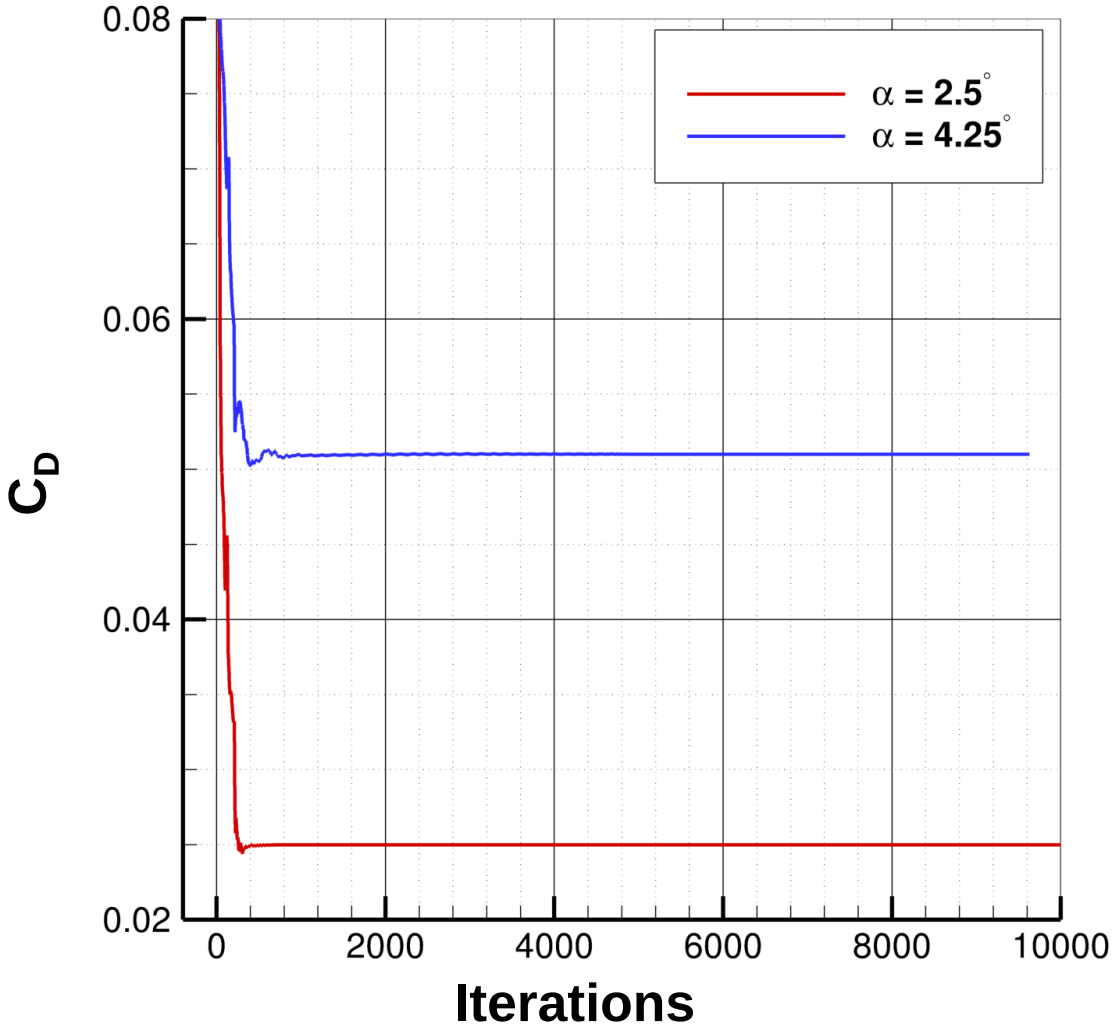
- **Flow conditions**
  - Mach number: $M = 0.85$
  - Reynolds number: $Re = 20 \text{ million}$
  - reference temperature: $T_{ref} = -250\ °F$
  - $C_L = 0.5,\ \alpha = 2.5°,\ 2.75°,\ 3.00°,\ 3.25°,\ 3.50°,\ 3.75°,\ 4.00°,\ 4.25°$
- **USM3D-ME solutions**
  - rapid iterative convergence
  - solution residuals reduced below 1.0E-13

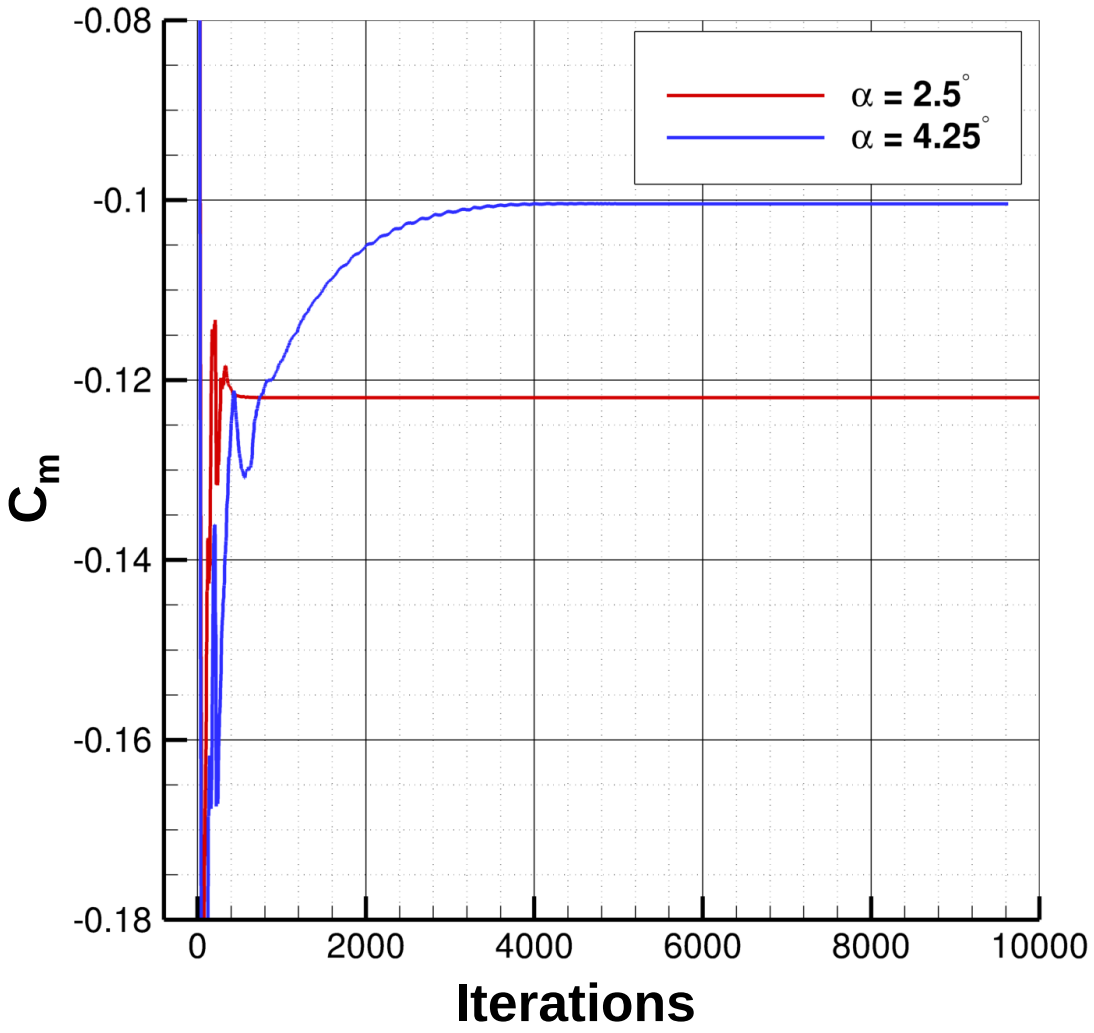
Case 2a: Iterative Convergence





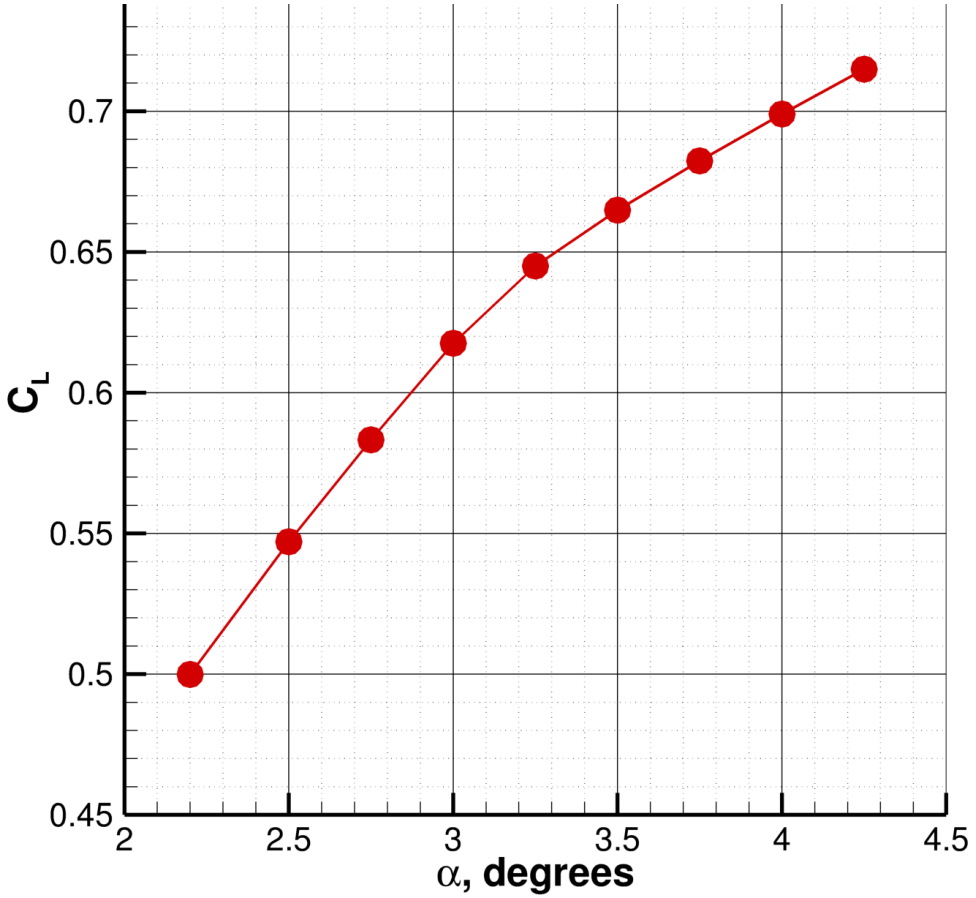
Case 2a: Iterative Convergence (cont.)

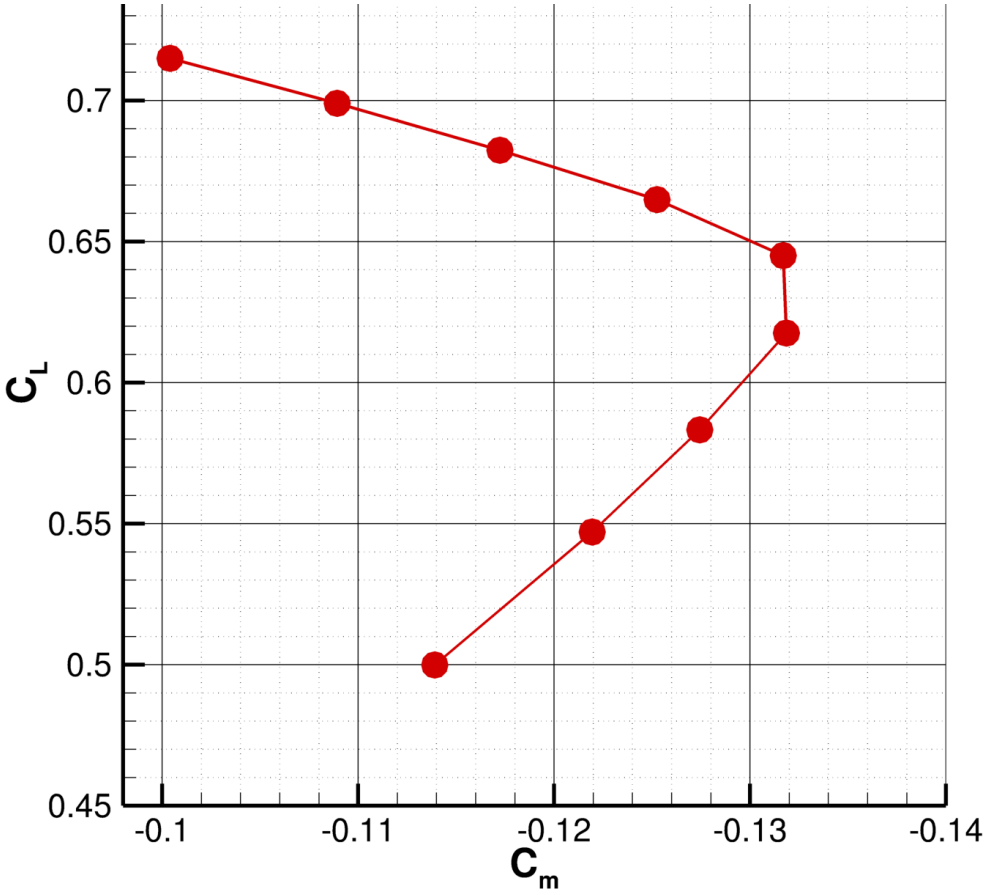




Case 2a: Aerodynamic Performance

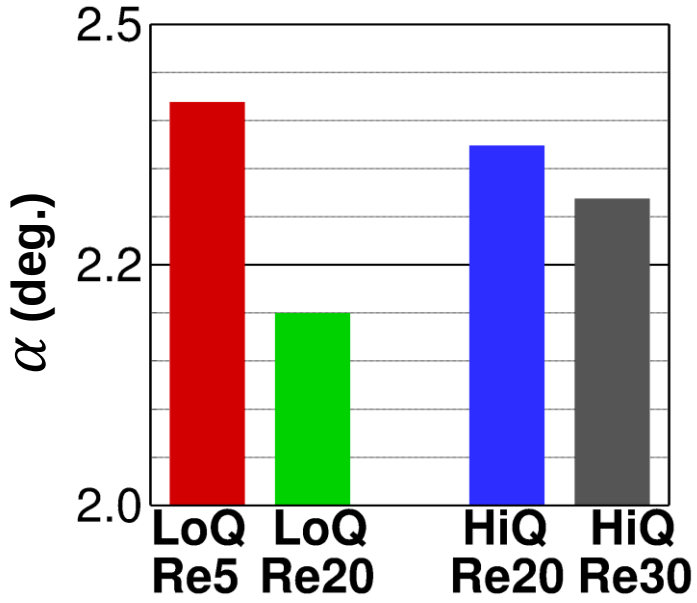
- Pitch break observed for $0.62 \leq C_L \leq 0.65$ ($3° \leq \alpha \leq 3.25°$)
- Bucket of pitching moment curve at $C_M \approx -0.133$

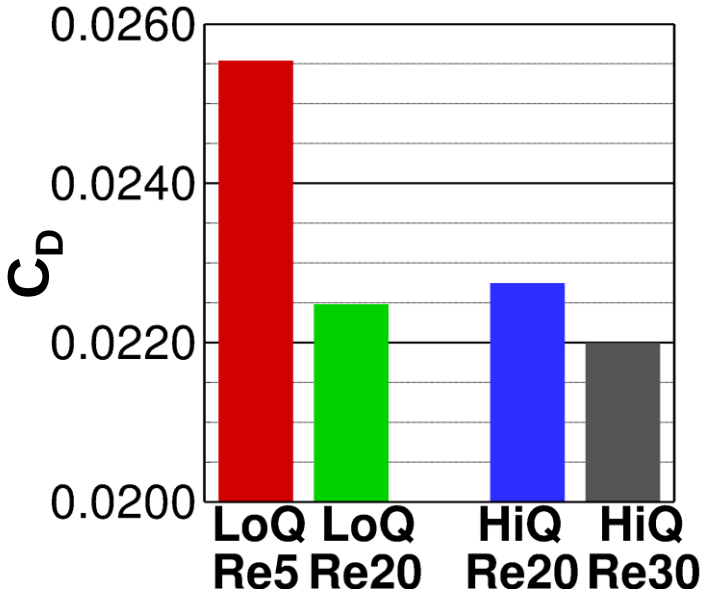


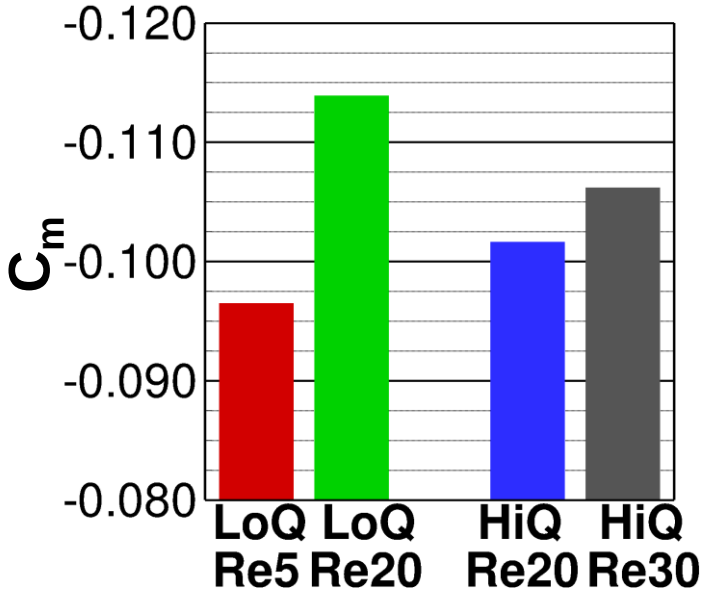


Case 3: Reynolds Number Sweep

- **Flow conditions**
  - $M = 0.85,\ C_L = 0.5,\ Re = 5$ million, $T_{ref} = 100\ °F, \alpha = 2.5°,$ LoQ AE
  - $M = 0.85,\ C_L = 0.5,\ Re = 20$ million, $T_{ref} = -250\ °F, \alpha = 2.5°,$ LoQ AE
  - $M = 0.85,\ C_L = 0.5,\ Re = 20$ million, $T_{ref} = -182\ °F, \alpha = 2.5°,$ HiQ AE
  - $M = 0.85,\ C_L = 0.5,\ Re = 30$ million, $T_{ref} = -250\ °F, \alpha = 2.5°,$ HiQ AE
- **Drag increases with lower Reynolds number as wing moves off design**







Conclusions

- **New implementation of SA-neg turbulence model in USM3D-ME improved robustness**
- **DPW-VII solutions for cases 1a, 2a, and 3 presented**
  - sectional cuts for pressure and skin friction, surface pressure, and streamlines in paper
- **Rapid convergence to machine-zero residuals achieved in all computations**
- **Strong grid convergence using six JAXA grids**
- **Pitch break predicted at $C_L \approx 0.63$ ($\alpha \approx 3.15°$)**

Acknowledgments

- NASA Transformative Tools and Technologies (TTT) project of Transformative Aeronautics Concepts Program (TACP)
- NASA Commercial Supersonic Technology (CST) project of Advanced Air Vehicles Program (AAVP)
- DPW-VII workshop committee for providing grids, data format, and data reduction scripts
- Computations conducted on NAS supercomputing facility

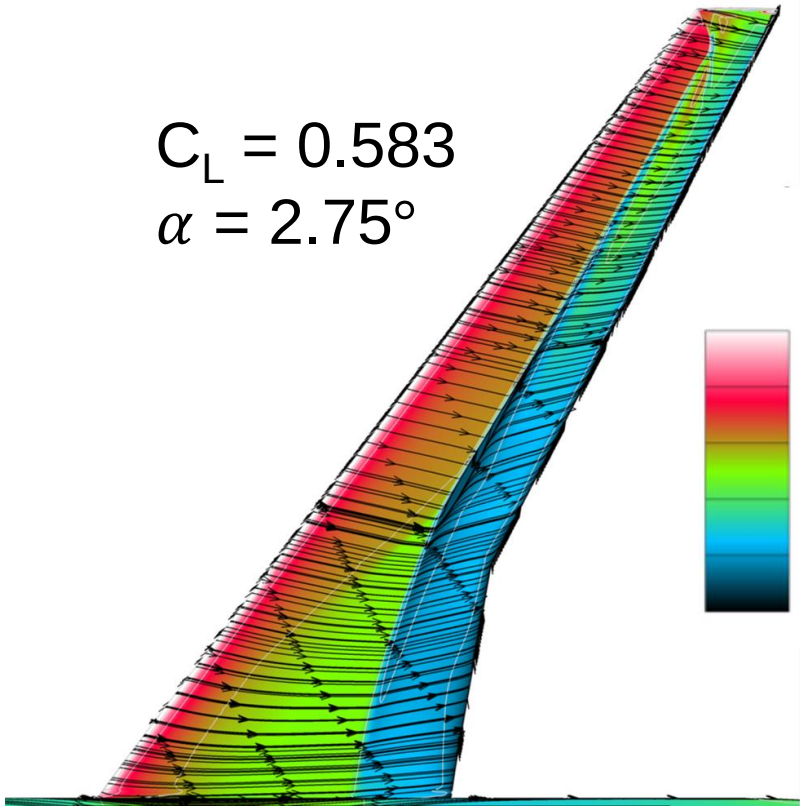

CFD DRAG PREDICTION WORKSHOP SERIES
DPW
ESTABLISHED 2000

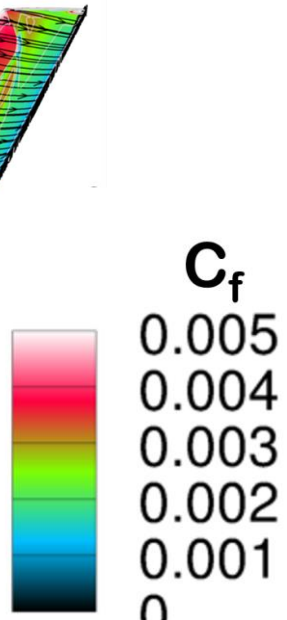
Case 2a: Surface Separation Behavior

- **Surface contours of C_f with streamlines**
- **Shock-induced separation observed at α = 3.00°**
- **Midspan separation seen at α = 3.25°**

$M = 0.85$
$Re = 20$ million
$T_{ref} = -250\ °F$

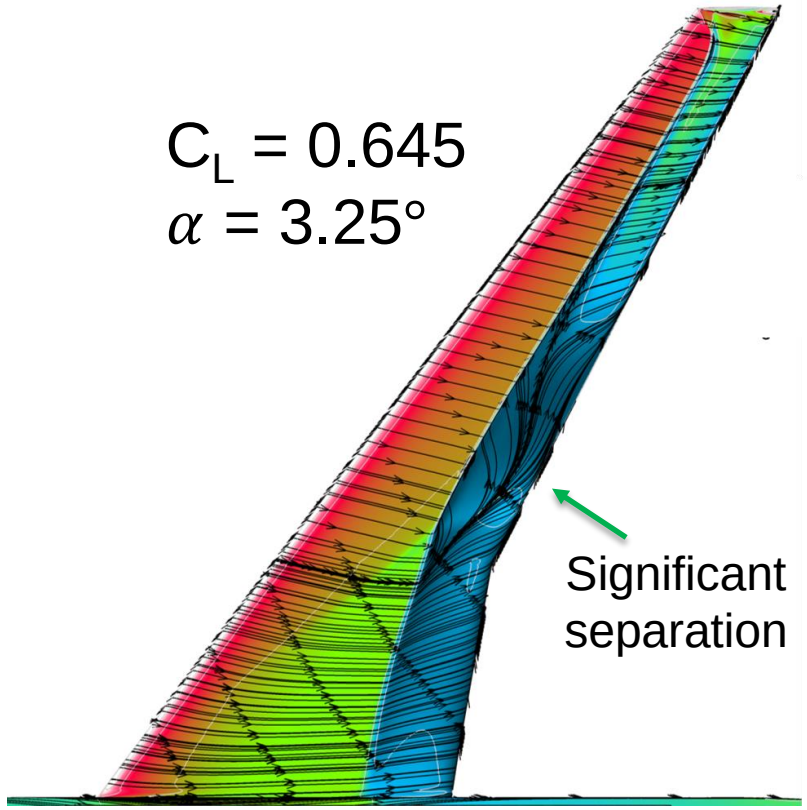
C_L = 0.583
α = 2.75°





C_L = 0.618
α = 3.00°

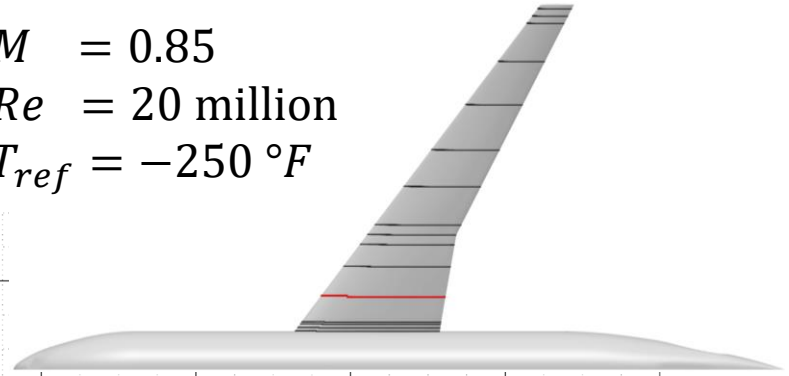
C_L = 0.645
α = 3.25°

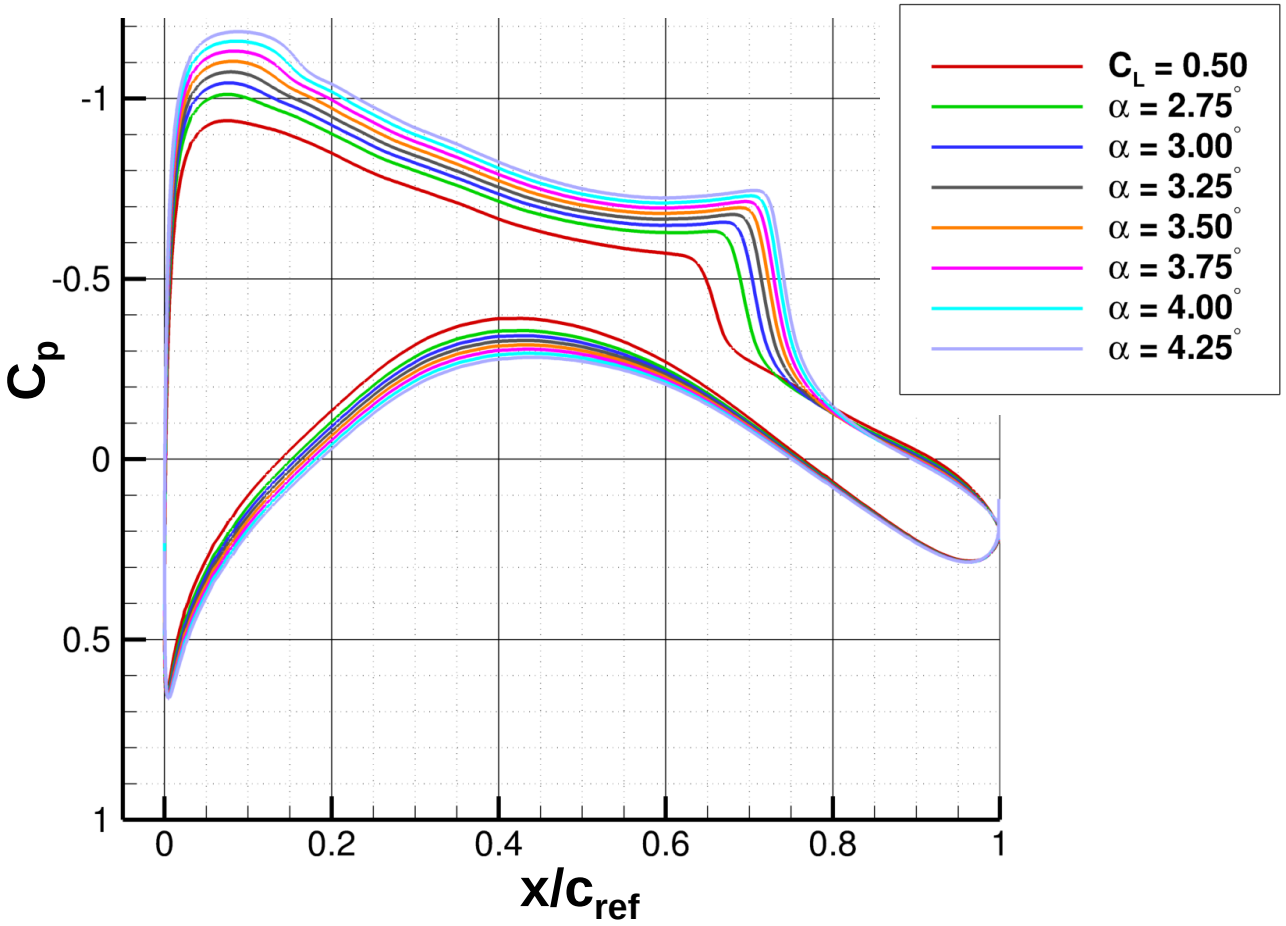


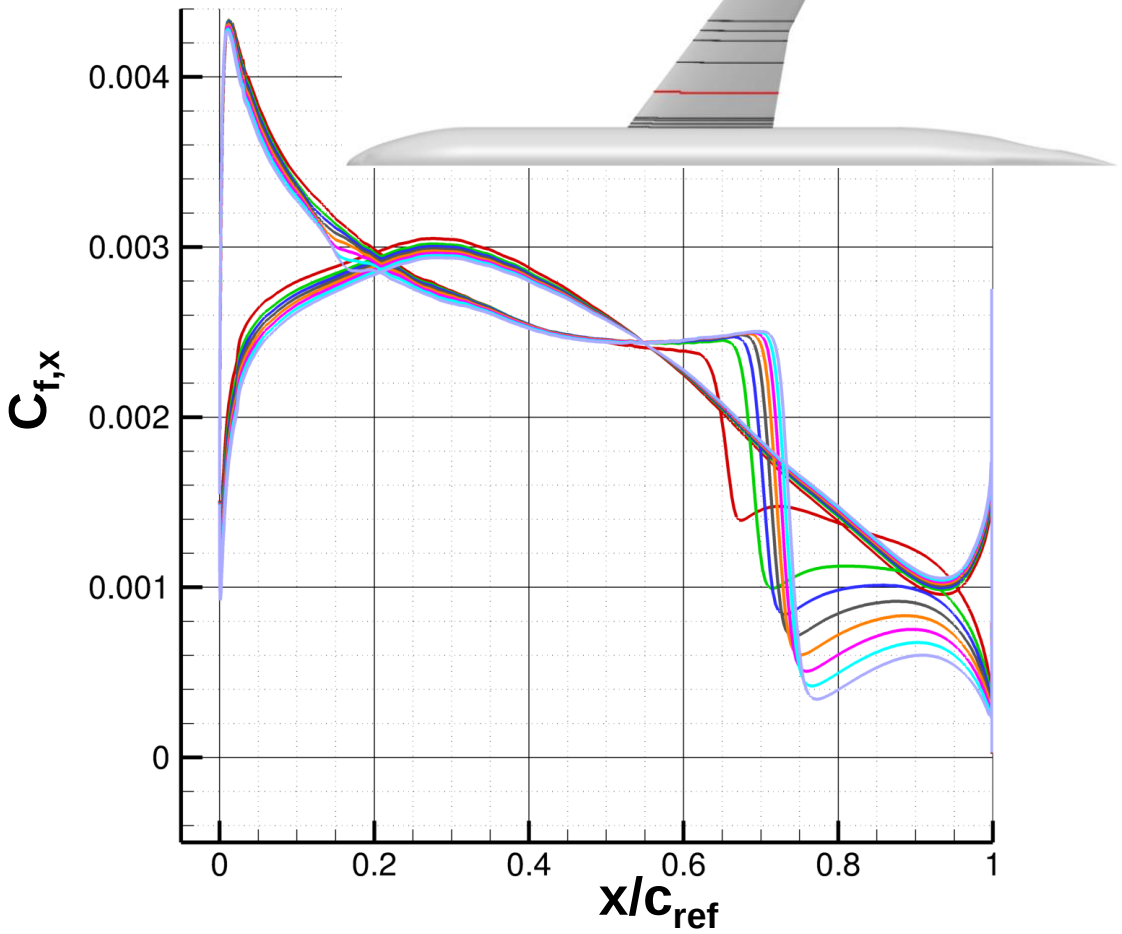
Case 2a: Inboard Surface Cuts ($\eta = 0.201$)

- **Attached flow present across all simulations**

$M = 0.85$
$Re = 20$ million
$T_{ref} = -250\ °F$



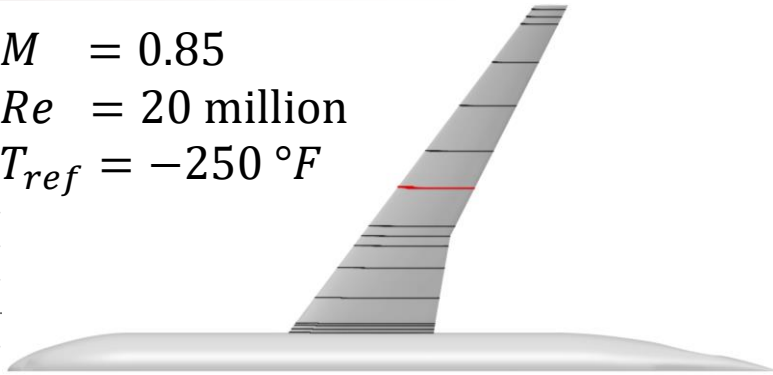


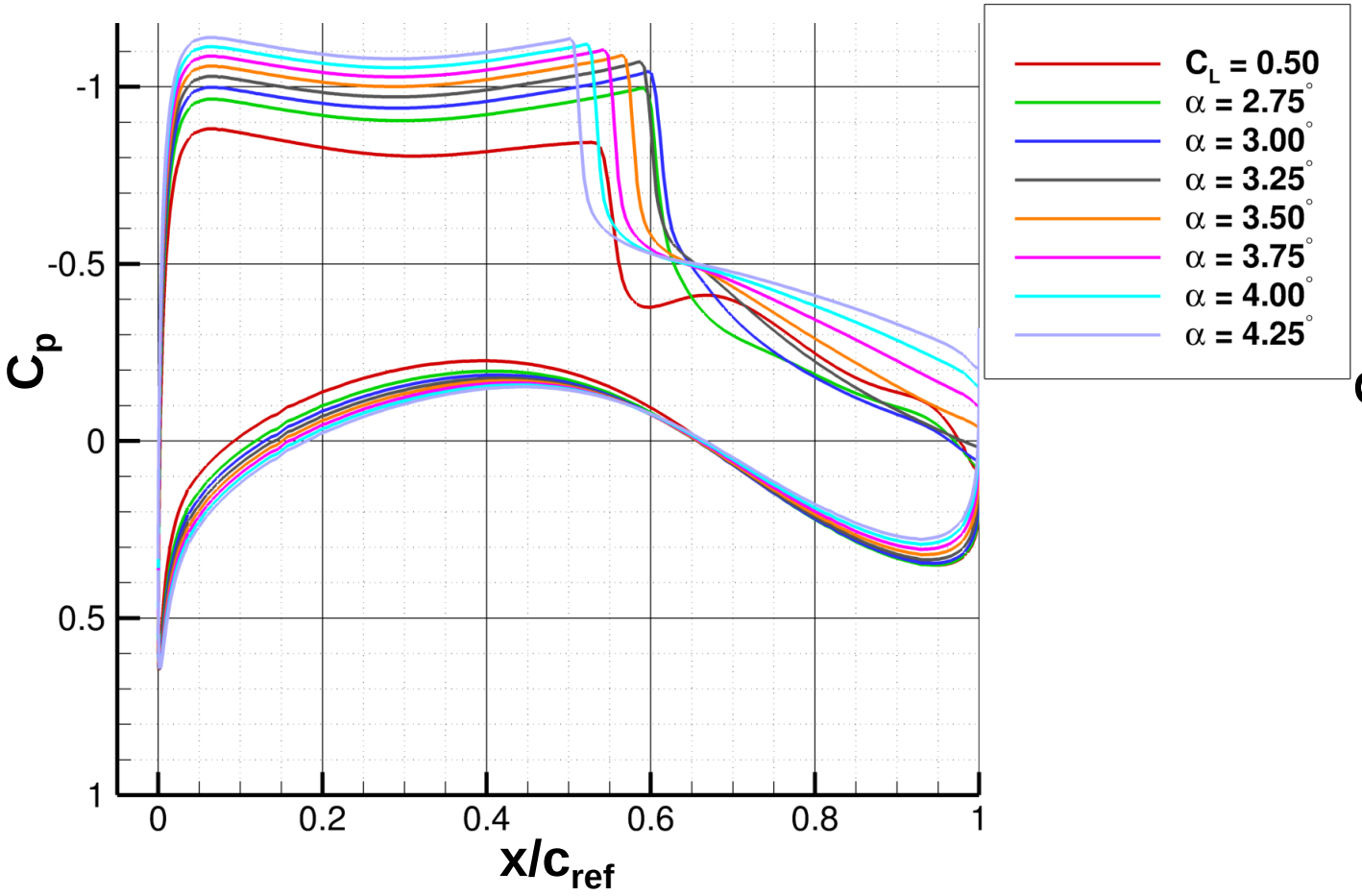


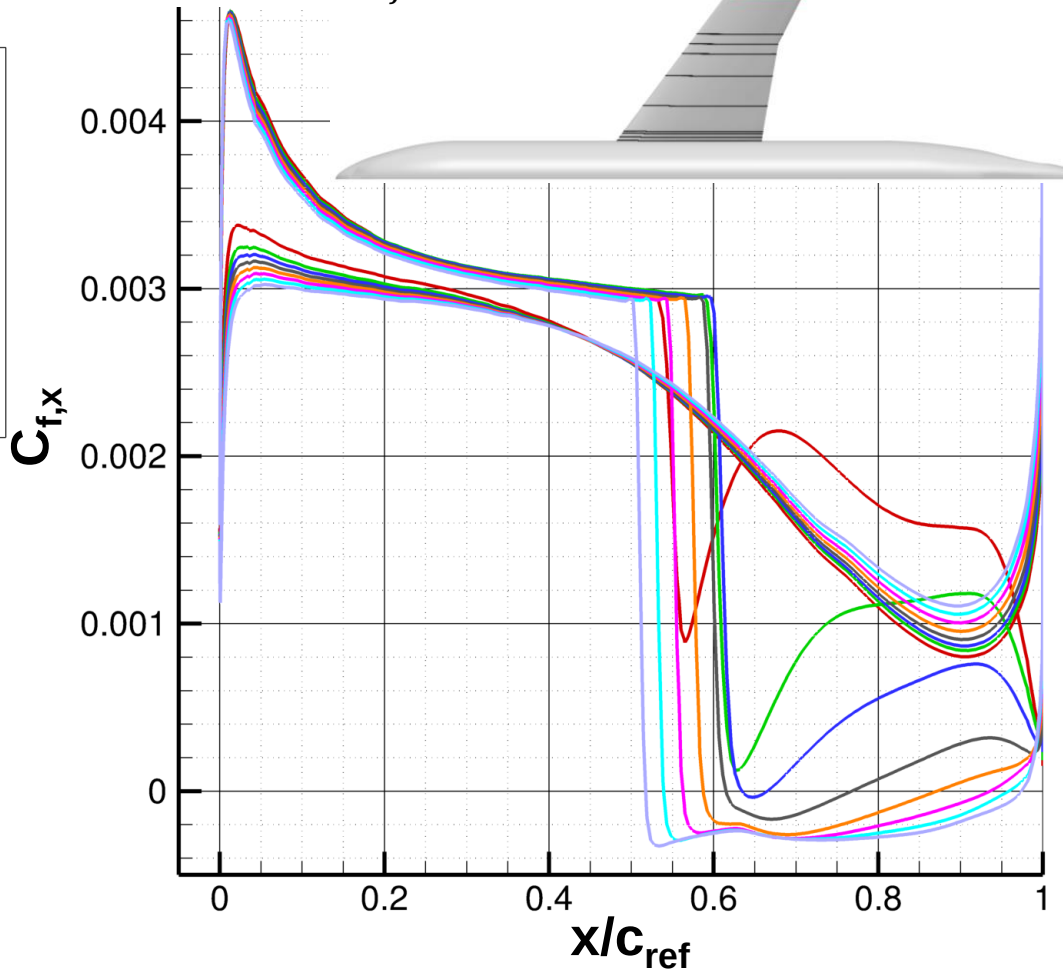
Case 2a: Midspan Surface Cuts ($\eta = 0.502$)

- **Trailing edge separation for $\alpha \geq 3.0°$**
- **Separation increases with larger angles of attack**

$M = 0.85$
$Re = 20$ million
$T_{ref} = -250\ °F$





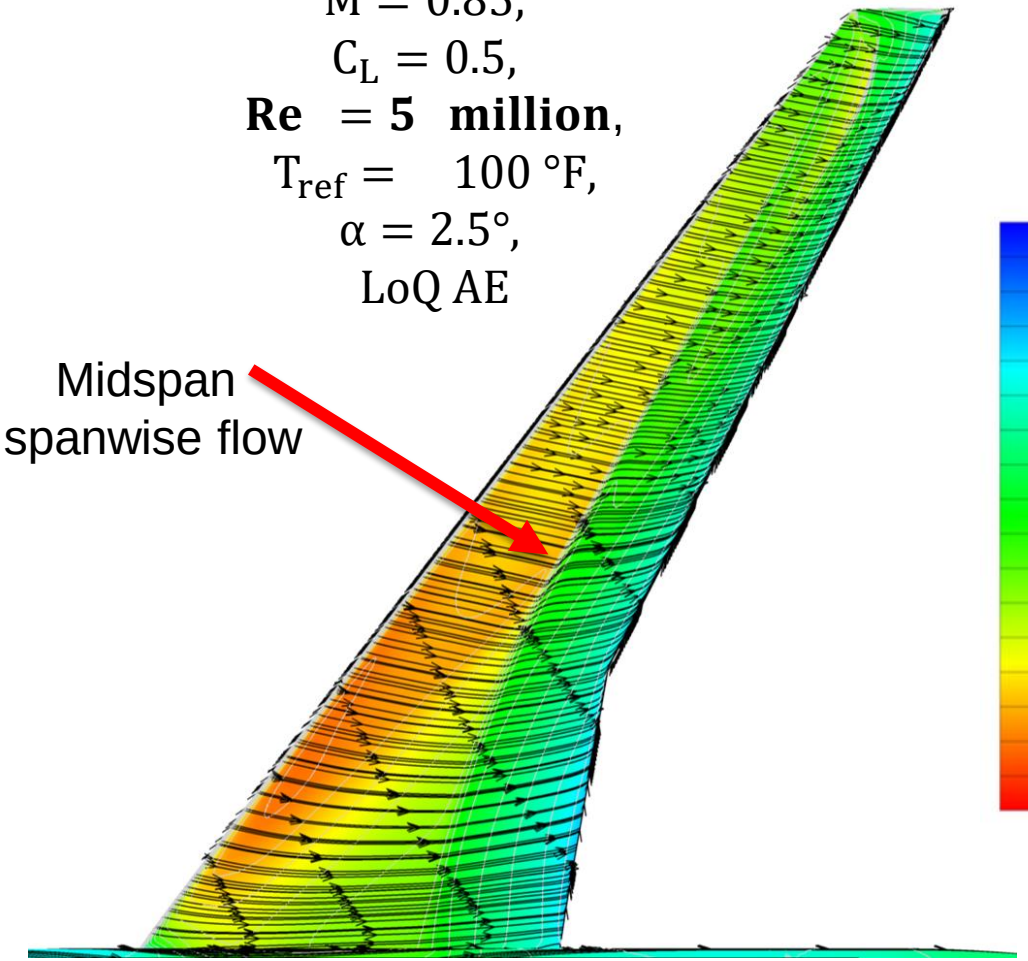


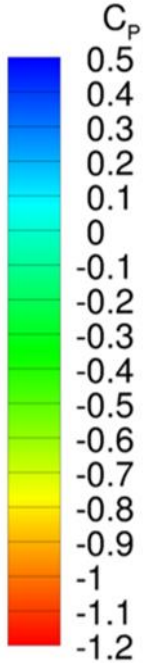
Case 3: Surface Pressure Comparison

- **Localized spanwise flow observed for low-Reynolds number case**

$M = 0.85$,
$C_L = 0.5$,
Re = 5 million,
$T_{ref} = 100\ °F$,
$\alpha = 2.5°$,
LoQ AE

Midspan spanwise flow





$M = 0.85$,
$C_L = 0.5$,
Re = 30 million,
$T_{ref} = -250\ °F$,
$\alpha = 2.5°$,
HiQ AE

